

# A large-area multi-finger $\beta$ -Ga<sub>2</sub>O<sub>3</sub> MOSFET and its self-heating effect

Xuanze Zhou, Guangwei Xu<sup>†</sup>, and Shibing Long<sup>†</sup>

School of Microelectronics, University of Science and Technology of China, Hefei 230026, China

**Abstract:** The self-heating effect severely limits device performance and reliability. Although some studies have revealed the heat distribution of  $\beta$ -Ga<sub>2</sub>O<sub>3</sub> MOSFETs under biases, those devices all have small areas and have difficulty reflecting practical conditions. This work demonstrated a multi-finger  $\beta$ -Ga<sub>2</sub>O<sub>3</sub> MOSFET with a maximum drain current of 0.5 A. Electrical characteristics were measured, and the heat dissipation of the device was investigated through infrared images. The relationship between device temperature and time/bias is analyzed.

**Key words:**  $\beta$ -Ga<sub>2</sub>O<sub>3</sub>; MOSFET; multi-finger; self-heating effect

**Citation:** X Z Zhou, G W Xu, and S B Long, A large-area multi-finger  $\beta$ -Ga<sub>2</sub>O<sub>3</sub> MOSFET and its self-heating effect[J]. *J. Semicond.*, 2023, 44(7), 072804. <https://doi.org/10.1088/1674-4926/44/7/072804>

## 1. Introduction

Ultra-wide bandgap  $\beta$ -Ga<sub>2</sub>O<sub>3</sub> is a promising candidate for advanced high-power applications owing to its outstanding material properties, including a large bandgap of  $\sim 4.8$  eV, a high critical breakdown field of 8 MV/cm and a large Baliga's figure of merit of 3444<sup>[1, 2]</sup>. Low-cost and scalable melting growth techniques such as edge-defined film-fed growth (EFG)<sup>[3]</sup> and Czochralski<sup>[4]</sup> methods give advantages to  $\beta$ -Ga<sub>2</sub>O<sub>3</sub> over other wide bandgap materials such as SiC, GaN and diamond. Among these material properties of  $\beta$ -Ga<sub>2</sub>O<sub>3</sub>, low thermal conductivity (11–27 W/(m·K) at 300 K) can cause a severe self-heating effect (SHE) and affect device reliability and stability<sup>[5]</sup>.

$\beta$ -Ga<sub>2</sub>O<sub>3</sub> power metal–oxide–semiconductor field-effect transistors (MOSFETs) have been investigated since 2012<sup>[6]</sup> and have achieved remarkable results<sup>[7–11]</sup>. Constructive methods have been proposed to minimize the SHE of  $\beta$ -Ga<sub>2</sub>O<sub>3</sub> MOSFETs<sup>[12, 13]</sup>, such as the ion-cutting technique<sup>[14]</sup>, transfer to a foreign substrate<sup>[15, 16]</sup> and structural design<sup>[17]</sup>. Novel measurements have been used to characterize the transient temperature distribution of  $\beta$ -Ga<sub>2</sub>O<sub>3</sub> MOSFETs<sup>[18]</sup>. Most reports on  $\beta$ -Ga<sub>2</sub>O<sub>3</sub>-based MOSFETs have focused on pursuing high PFOMs and exploring novel structures, yet large-area structures are needed to sustain a high on-state current for practical applications. For large-area structures, SHE will be more serious compared with small devices because of the smaller surface area-to-volume ratio, which is worth investigating. The main challenge of fabricating high performance large-area  $\beta$ -Ga<sub>2</sub>O<sub>3</sub> transistor is the inhomogeneity of material growth and instable process flow. There have been reports that multi-finger  $\beta$ -Ga<sub>2</sub>O<sub>3</sub> MOSFETs are capable of delivering 300 V switching transients with voltage slopes reach up to 65 V/ns<sup>[19]</sup>, showing great potential. Nonetheless, the electri-

cal and thermal properties of this technology remain to be thoroughly explored. In this work, we fabricated a multi-fingers  $\beta$ -Ga<sub>2</sub>O<sub>3</sub> MOSFET with output current reach to 0.5 A. DC characteristics have been studied. We have employed optical thermography to investigate the impact of the self-heating effect on the multi-finger  $\beta$ -Ga<sub>2</sub>O<sub>3</sub> MOSFET.

## 2. Experiment

A semi-insulating Fe-doped (010)  $\beta$ -Ga<sub>2</sub>O<sub>3</sub> bulk substrate was used in this work. A  $\beta$ -Ga<sub>2</sub>O<sub>3</sub> film with a concentration of  $\sim 2 \times 10^{17}$  cm<sup>-3</sup> was grown on the substrate by MOCVD. Before film growth, a 30-min wafer carrier bake was performed for cleaning at 860 °C. Details of growth and doping can be found in our previous report. Fig. 1 shows the cross-sectional schematic of the fabricated  $\beta$ -Ga<sub>2</sub>O<sub>3</sub> MOSFET. The fabrication process started with mesa isolation was performed by BCl<sub>3</sub>/Ar inductively coupled plasma (ICP) dry etching. Then, 300 nm of SiO<sub>2</sub> was grown by plasma-enhanced chemical vapor deposition (PECVD) at 300 °C, and source/drain areas were exposed by buffered oxide etching (BOE) for regrowth of the heavily doped ohmic contact region by MOCVD. After that, SiO<sub>2</sub> was fully removed by hydrofluoric acid solution for over 30 min. The Ti/Au (20/180 nm) metal stack was then deposited by electron beam evaporation and subjected to rapid thermal annealing at 470 °C for 1 min in a nitrogen atmosphere. Thereafter, 30 nm thick Al<sub>2</sub>O<sub>3</sub> was deposited as the gate dielectric layer by atomic layer deposition (ALD) at 250 °C, and pad regions were opened by removing Al<sub>2</sub>O<sub>3</sub> using ICP etching. Finally, Ni/Au (20/80 nm) gate metal was deposited by electron beam evaporation. Small-area transistors with a gate width ( $W_g$ ) of 10  $\mu$ m, a gate-to-source distance ( $L_{gs}$ ) of 2  $\mu$ m, a gate-to-drain distance ( $L_{gd}$ ) of 7  $\mu$ m and a gate length ( $L_g$ ) of 2  $\mu$ m were fabricated to evaluate the device properties. The device temperature distribution was characterized by a Fluke TiX580 infrared thermal imaging camera.

## 3. Results and discussion

The DC characteristics of the small-area transistor were

Correspondence to: G W Xu, [xugw@ustc.edu.cn](mailto:xugw@ustc.edu.cn); S B Long, [shibinglong@ustc.edu.cn](mailto:shibinglong@ustc.edu.cn)

Received 31 DECEMBER 2022; Revised 20 FEBRUARY 2023.

©2023 Chinese Institute of Electronics

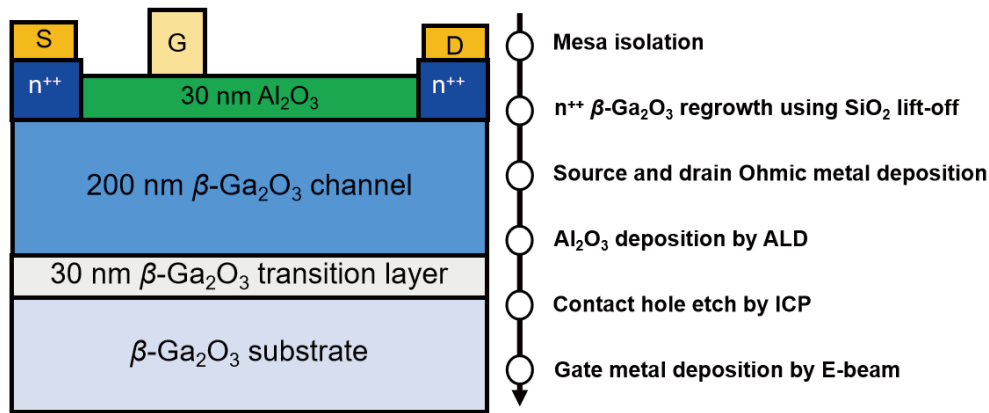


Fig. 1. (Color online) Cross-sectional schematic of the  $\beta$ -Ga<sub>2</sub>O<sub>3</sub> MOSFET and its process flow.

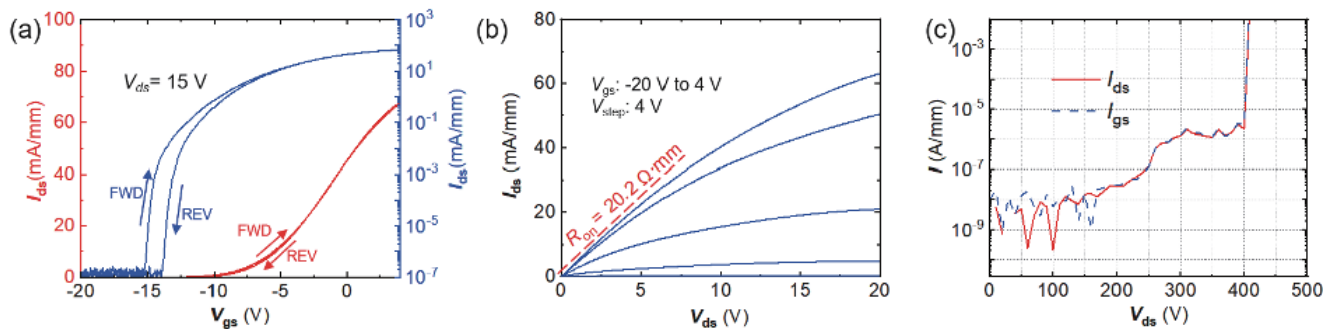


Fig. 2. (Color online) DC (a) transfer and (b) output characteristics of small-area MOSFET. (c) Three terminal leakage current under the off-state.

determined by a Keysight B1500A semiconductor device analyzer. Fig. 2(a) shows the transfer characteristics of the small-area MOSFET. A threshold voltage  $V_{th} = -11$  V, subthreshold swing  $SS = 190$  mV/dec and an on/off ratio  $I_{on}/I_{off} > 10^8$  were extracted. Fig. 2(b) illustrates the output characteristics of the small-area MOSFET. The saturation drain-source current  $I_{ds} = 63$  mA/mm and on-state resistance  $R_{on} = 20.2$   $\Omega$ -mm were obtained. Fig. 2(c) shows the off-state characteristics of the small-area device, which was carried out by a Keysight B1505A power device analyzer. Gate bias was kept at  $-15$  V during the test. A three-terminal breakdown voltage of 400 V was obtained.

Figs. 3(a) and 3(b) give an optical microscope image of a multi-finger  $\beta$ -Ga<sub>2</sub>O<sub>3</sub> MOSFET and its layout. The multi-finger MOSFET featured a finger-to finger distance of 20  $\mu$ m, which is composed of  $L_{gs} = 4$   $\mu$ m,  $L_g = 4$   $\mu$ m and  $L_{gd} = 12$   $\mu$ m. Each finger has a width of 20  $\mu$ m. The large-area transistor showed an on-state current of 0.5 A and an on-resistance of 13  $\Omega$ , as shown in Fig. 3(d). The different threshold voltages between large-area and small-area devices can be ascribed to epitaxial  $\beta$ -Ga<sub>2</sub>O<sub>3</sub> film. The current and voltage level is still lagging behind the small-area device due to uniformity issues in material growth and the device fabrication process. Upon the establishment of mature material growth and fabrication process, the inherent advantages of the material can be fully demonstrated.

The temperature distribution images measured by the infrared camera are shown in Figs. 4(a)–4(d). The gate electrode was kept floating during the test. According to the results, the heat was mainly generated in the  $\beta$ -Ga<sub>2</sub>O<sub>3</sub> channel between the source and drain and then mainly dissipated through the metals, which explains why the metal pos-

sessed a lower temperature during the tests. This phenomenon became more obvious in the thermal equilibrium state (see Fig. 5(a)). The maximum temperature in the  $\beta$ -Ga<sub>2</sub>O<sub>3</sub> channel almost reached 250  $^{\circ}$ C under an applied voltage of 8 V, showing the severe self-heating effect of the large-area transistor. The primary reason for the comparatively reduced temperature of the metal pad is primarily ascribed to its superior conductivity in comparison to  $\beta$ -Ga<sub>2</sub>O<sub>3</sub>. It is worth noting that the reflectivity and emissivity of the metal surface could potentially impact the precision of temperature measurement. To alleviate SHE, effective cooling mechanisms are necessary to regulate the SHE, including the implementation of high-thermal-conductivity carrier wafers<sup>[15]</sup> for top-side or flip-chip integration<sup>[20]</sup>, as well as the utilization of heat sinks<sup>[12]</sup>.

## 4. Conclusion

In summary, we present a multi-finger  $\beta$ -Ga<sub>2</sub>O<sub>3</sub> MOSFET with a saturation current over 0.5 A. The self-heating effect was investigated by infrared images. The generation and dissipation actions were analyzed. This work provides a better understanding of the self-heating effect of large-area  $\beta$ -Ga<sub>2</sub>O<sub>3</sub> MOSFETs and is significant for high-power applications.

## Acknowledgements

This work was supported by the National Natural Science Foundation of China (NSFC) under Grant Nos. 61925110, 62004184 and 62234007, the Key-Area Research and Development Program of Guangdong Province under Grant No. 2020B010174002. This work was partially carried out at the Center for Micro and Nanoscale Research and Fabrication of University of Science and Technology of China (USTC).

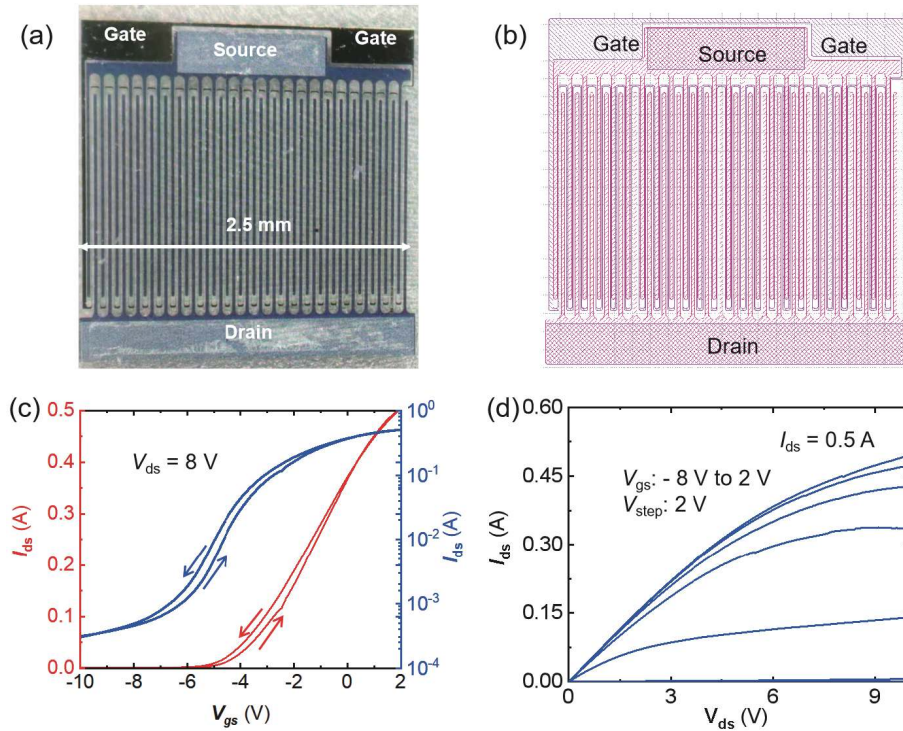


Fig. 3. (Color online) (a) Optical microscope image and (b) layout of a multi-finger  $\beta$ -Ga<sub>2</sub>O<sub>3</sub> MOSFET. (c) Transfer and (d) output characteristics of multi-finger MOSFET.

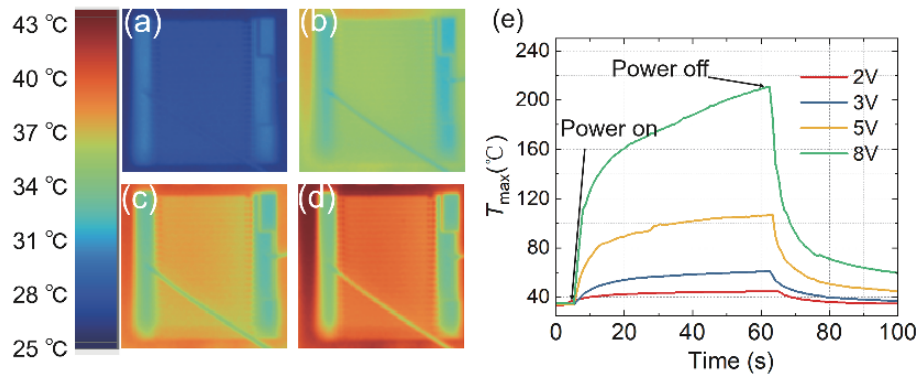


Fig. 4. (Color online) Temperature distribution images with biased time of (a) 0 s, (b) 10 s, (c) 20 s and (d) 50 s. The drain bias was set as 2 V. (e) Time dependence of the maximum temperature in the  $\beta$ -Ga<sub>2</sub>O<sub>3</sub> channel with different drain voltages.

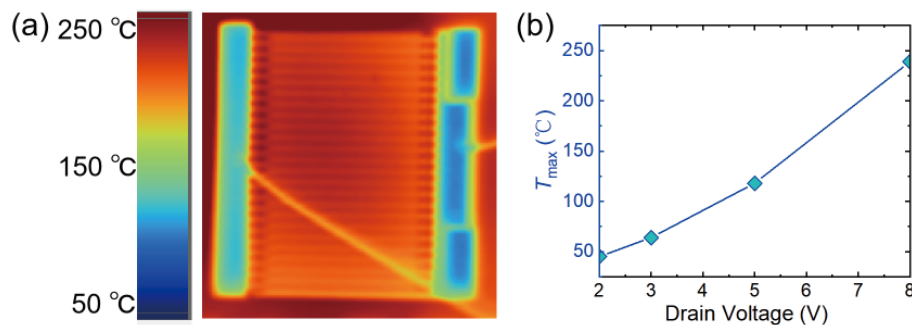


Fig. 5. (Color online) Thermal equilibrium state: (a) temperature distribution image with a drain voltage of 8 V and (b) maximum temperature in the  $\beta$ -Ga<sub>2</sub>O<sub>3</sub> channel versus applied drain voltage.

## References

- [1] Higashiwaki M, Sasaki K, Murakami H, et al. Recent progress in Ga<sub>2</sub>O<sub>3</sub> power devices. *Semicond Sci Technol*, 2016, 31, 034001
- [2] Dong H, Xue H W, He Q M, et al. Progress of power field effect transistor based on ultra-wide bandgap Ga<sub>2</sub>O<sub>3</sub> semiconductor material. *J Semicond*, 2019, 40, 011802
- [3] Kuramata A, Koshi K, Watanabe S, et al. High-quality  $\beta$ -Ga<sub>2</sub>O<sub>3</sub> single crystals grown by edge-defined film-fed growth. *Jpn J Appl Phys*, 2016, 55, 1202A2
- [4] Tomm Y, Reiche P, Klimm D, et al. Czochralski grown Ga<sub>2</sub>O<sub>3</sub> crystals. *J Cryst Growth*, 2000, 220, 510

- [5] Yu Y T, Xiang X Q, Zhou X Z, et al. Device topological thermal management of  $\beta$ -Ga<sub>2</sub>O<sub>3</sub> Schottky barrier diodes. *Chin Phys B*, 2021, 30, 067302
- [6] Higashiwaki M, Sasaki K, Kuramata A, et al. Gallium oxide (Ga<sub>2</sub>O<sub>3</sub>) metal-semiconductor field-effect transistors on single-crystal  $\beta$ -Ga<sub>2</sub>O<sub>3</sub> (010) substrates. *Appl Phys Lett*, 2012, 100, 013504
- [7] Liu H Y, Li J N, Lv Y J, et al. Improved electrical performance of lateral  $\beta$ -Ga<sub>2</sub>O<sub>3</sub> MOSFETs utilizing slanted fin channel structure. *Appl Phys Lett*, 2022, 121, 202101
- [8] Bhattacharyya A, Ranga P, Roy S, et al. Multi-kV class  $\beta$ -Ga<sub>2</sub>O<sub>3</sub> MESFETs with a lateral figure of merit up to 355 MW/cm<sup>2</sup>. *IEEE Electron Device Lett*, 2021, 42, 1272
- [9] Zhou X Z, Ma Y J, Xu G W, et al. Enhancement-mode  $\beta$ -Ga<sub>2</sub>O<sub>3</sub> U-shaped gate trench vertical MOSFET realized by oxygen annealing. *Appl Phys Lett*, 2022, 121, 223501
- [10] Wang C L, Zhou H, Zhang J C, et al. Hysteresis-free and  $\mu$ S-switching of D/E-modes Ga<sub>2</sub>O<sub>3</sub> hetero-junction FETs with the BV<sup>2</sup>/R<sub>on,sp</sub> of 0.74/0.28 GW/cm<sup>2</sup>. *Appl Phys Lett*, 2022, 120, 112101
- [11] Zhou X, Liu Q, Hao W, et al. Normally-off  $\beta$ -Ga<sub>2</sub>O<sub>3</sub> power hetero-junction field-effect-transistor realized by p-NiO and recessed gate. *IEEE 26th Int Symp Power Semiconductor Devices IC's (ISPSD)*, 2022
- [12] Kim S, Zhang Y W, Yuan C, et al. Thermal management of  $\beta$ -Ga<sub>2</sub>O<sub>3</sub> current aperture vertical electron transistors. *IEEE Trans Compon, Packag Manuf Technol*, 2021, 11, 1171
- [13] Chatterjee B, Zeng K, Nordquist C D, et al. Device-level thermal management of gallium oxide field-effect transistors. *IEEE Trans Compon Packag Manuf Technol*, 2019, 9, 2352
- [14] Xu W H, Wang Y B, You T G, et al. First demonstration of wafer-scale heterogeneous integration of Ga<sub>2</sub>O<sub>3</sub> MOSFETs on SiC and Si substrates by ion-cutting process. *2019 IEEE International Electron Devices Meeting (IEDM)*, 2019, 12
- [15] Noh J, Alajlouni S, Tadjer M J, et al. High performance  $\beta$ -Ga<sub>2</sub>O<sub>3</sub> nano-membrane field effect transistors on a high thermal conductivity diamond substrate. *IEEE J Electron Devices*, 2019, 7, 914
- [16] Zhou H, Maize K, Noh J, et al. Thermodynamic studies of Ga<sub>2</sub>O<sub>3</sub> nanomembrane field-effect transistors on a sapphire substrate. *ACS Omega*, 2017, 2, 7723
- [17] Chatterjee B, Li W, Nomoto K, et al. Thermal design of multi-fin Ga<sub>2</sub>O<sub>3</sub> vertical transistors. *Appl Phys Lett*, 2021, 119, 103502
- [18] Kumar N, Vaca D, Joishi C, et al. Ultrafast thermoreflectance imaging and electrothermal modeling of  $\beta$ -Ga<sub>2</sub>O<sub>3</sub> MESFETs. *IEEE Electron Device Lett*, 2020, 41, 641
- [19] Böcker J, Tetzner K, Heucke S, et al. Dispersion effects in on-state resistance of lateral Ga<sub>2</sub>O<sub>3</sub> MOSFETs at 300 V switching. *Electron Lett*, 2020, 56, 838
- [20] Gong H H, Zhou F, Yu X X, et al. 70- $\mu$ m-body Ga<sub>2</sub>O<sub>3</sub> Schottky barrier diode with 1.48 K/W thermal resistance, 59 A surge current and 98.9% conversion efficiency. *IEEE Electron Device Lett*, 2022, 43, 773



**Xuanze Zhou** got his BS from Nanchang University in 2018. Now he is a PhD student at University of Science and Technology of China under the supervision of Prof. Shibing Long and Dr. Guangwei Xu. His research focuses on gallium oxide power MOSFETs.



**Guangwei Xu** received his PhD from the Institute of Microelectronics of the Chinese Academy of Sciences in 2017. Then, he joined the University of California, Los Angeles as a postdoc. He joined the University of Science and Technology of China as an associate research fellow in the Shibing Long Group in 2019. His research focuses on wide bandgap semiconductor power device fabrication, device defect state measurement and device modeling.



**Shibing Long** is a full professor at the Institute of Microelectronics, University of Science and Technology of China. He received his PhD from the Institute of Microelectronics of the Chinese Academy of Sciences in 2005. Then, he worked there from 2005 to 2018 and joined the University of Science and Technology of China in 2018. His research focuses on micro- and nanofabrication, RRAM, ultrawide bandgap semiconductor devices (power devices and detectors) and memory circuit design.